Volume 17 | Number 43 | 21 November 2019 | Pages 9405–9538

Organic & Biomolecular Chemistry

rsc.li/obc

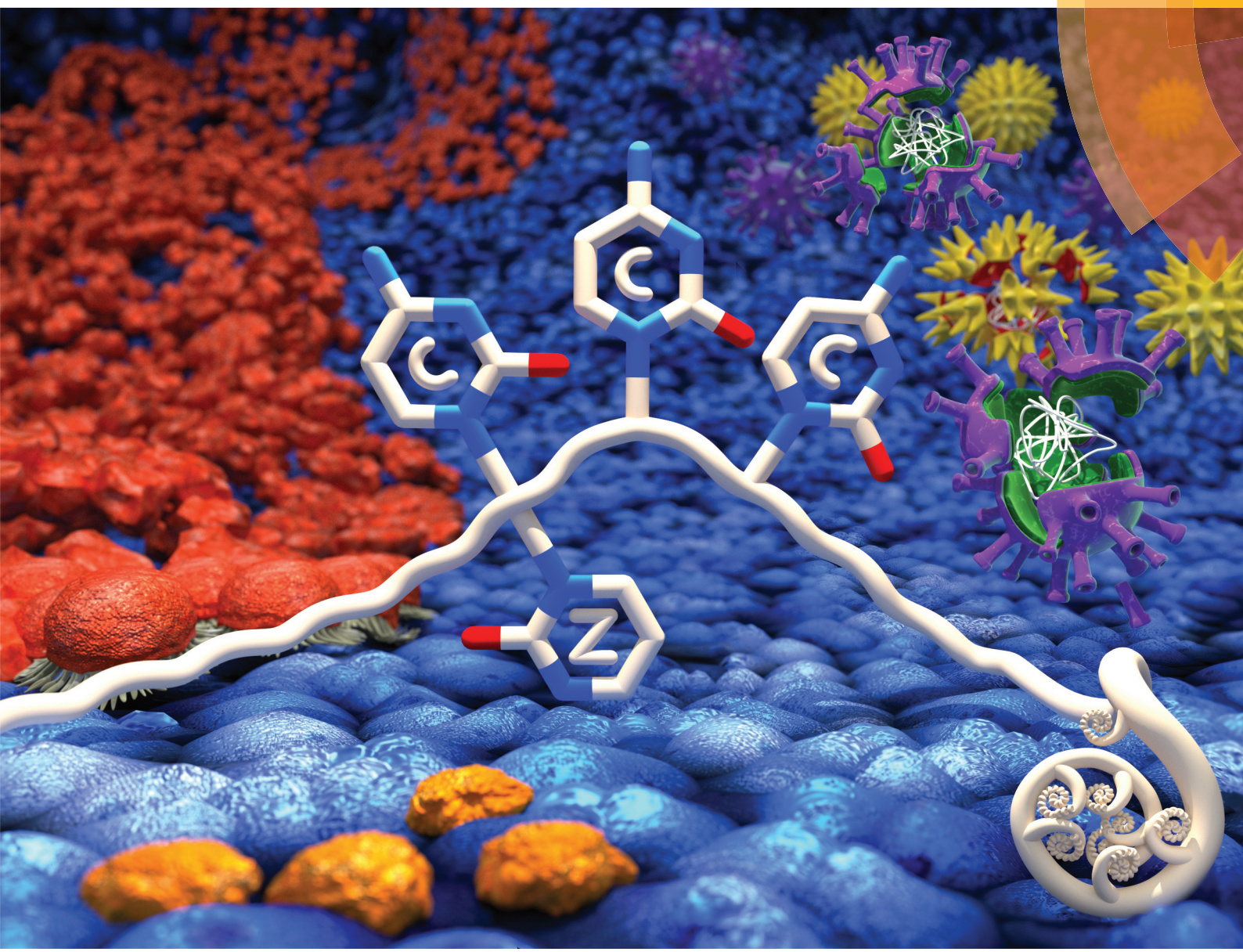

ISSN 1477-0520

ROYAL SOCIETY OF CHEMISTRY | Celebrating IYPT 2019

PAPER
Vyacheslav V. Filichev, Elena Harjes *et al.*
Selective inhibition of APOBEC3 enzymes by single-stranded DNAs containing 2′-deoxyzebularine

Organic & Biomolecular Chemistry

PAPER

View Article Online
View Journal | View Issue

Cite this: *Org. Biomol. Chem.*, 2019, **17**, 9435

Selective inhibition of APOBEC3 enzymes by single-stranded DNAs containing 2′-deoxyzebularine†

Fareeda M. Barzak, [a] Stefan Harjes,[a] Maksim V. Kvach, [a] Harikrishnan M. Kurup, [a,b] Geoffrey B. Jameson, [a,b] Vyacheslav V. Filichev *[a,b] and Elena Harjes *[a,b]

To restrict pathogens, in a normal human cell, APOBEC3 enzymes mutate cytosine to uracil in foreign single-stranded DNAs. However, in cancer cells, APOBEC3B (one of seven APOBEC3 enzymes) has been identified as the primary source of genetic mutations. As such, APOBEC3B promotes evolution and progression of cancers and leads to development of drug resistance in multiple cancers. As APOBEC3B is a non-essential protein, its inhibition can be used to suppress emergence of drug resistance in existing anti-cancer therapies. Because of the vital role of APOBEC3 enzymes in innate immunity, selective inhibitors targeting only APOBEC3B are required. Here, we use the discriminative properties of wild-type APOBEC3A, APOBEC3B and APOBEC3G to deaminate different cytosines in the CCC-recognition motif in order to best place the cytidine analogue 2′-deoxyzebularine (**dZ**) in the CCC-motif. Using several APOBEC3 variants that mimic deamination patterns of wild-type enzymes, we demonstrate that selective inhibition of APOBEC3B in preference to other APOBEC3 constructs is feasible for the dZCC motif. This work is an important step towards development of *in vivo* tools to inhibit APOBEC3 enzymes in living cells by using short, chemically modified oligonucleotides.

Received 13th August 2019,
Accepted 21st August 2019

DOI: 10.1039/c9ob01781j

rsc.li/obc

Introduction

The human APOBEC3 (A3A-H) protein family attacks retroviruses and other pathogens by hypermutating cytosine to uracil in single-stranded (ss)DNA (Fig. 1A).[1] Deaminase activity is dependent on a zinc-mediated hydrolytic mechanism, in which a conserved zinc-coordinating motif (His-X-Glu-X_{25-31}-Pro-Cys-X_{2-4}-Cys, X indicates any amino acid) serves to coordinate the zinc ion into the active site of the enzyme.[2–4] Besides targeting viruses[1] and retrotransposons,[5] several A3 enzymes, particularly A3A, A3B, and A3G, can deaminate cytosine in human nuclear and mitochondrial genomes.[6] This mutational activity of A3 proteins is recruited by viruses and cancer cells to increase the rates of mutagenesis, escape adaptive immune responses, and become drug resistant.[7–11] A3B is the major source of genetic mutations in multiple cancers (such as breast, bladder, cervix, lung, ovarian, head, and neck), and A3A and A3H are responsible for additional A3-dependent mutations.[9–15]

Because A3B is not an essential protein,[16] its inhibition may be used to supplement existing anticancer and retroviral therapies.[17] Due to the important role of A3 proteins for immune defence against pathogens, it is vital to specifically inhibit only one family member, in particular A3B, leaving others intact and active. The relative contribution of A3A and A3B to carcenogenesis is not clarified yet for many cancers.[15,18] However, A3A

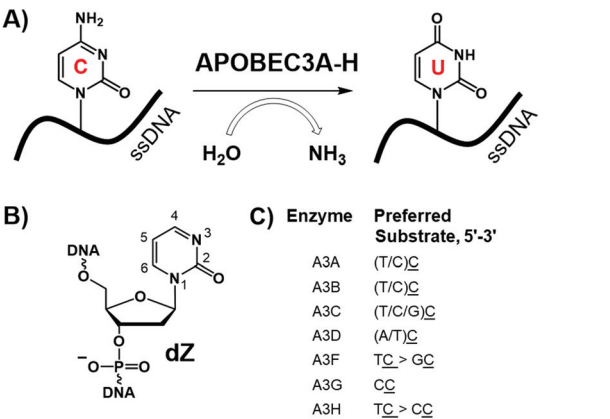

Fig. 1 (A) Deamination of dC in ssDNA by A3 enzymes; (B) inhibitor of cytidine deamination used in this work: 2′-deoxyzebularine (**dZ**) incorporated in the ssDNA; (C) preferred ssDNA substrates of A3 enzymes, where the underlined C is the preferred target (adapted from ref. 25).

[a]*School of Fundamental Sciences, Massey University, Private Bag 11 222, Palmerston North 4442, New Zealand*
[b]*Maurice Wilkins Centre for Molecular Biodiscovery, Auckland 1142, New Zealand.*
E-mail: e.harjes@massey.ac.nz, v.filichev@massey.ac.nz

†Electronic supplementary information (ESI) available. See DOI: 10.1039/c9ob01781j

is not expressed significantly and its activity is not detectable in breast cancer cell lines.[10,19,20] In contrast, A3B is the major source of mutations in multiple breast cancer cell lines.[19,20] Therefore, selective inhibition of A3B is important at least for treatment of breast cancers. In addition, selective inhibitors may provide *in vitro* and *in vivo* tools to address the mutagenic role of A3A and A3B in other cancers.

We have recently developed the first substrate-like competitive A3 inhibitors,[21] in which the target 2′-deoxycytidine (dC) in ssDNA (*e.g.*, 5′-ATTTCATTT) was substituted by 2′-deoxyzebularine (**dZ**, Fig. 1B), a known inhibitor for cytidine deamination by cytidine deaminases that accept only single nucleosides.[22,23] Protonation of N3 in **dZ** by the conserved glutamic acid present in the active site of A3s (and single nucleoside cytidine deaminase, CDA) activates C4 in **dZ** to accept nucleophilic OH^-/H_2O coordinated to the Zn^{2+}, thereby converting **dZ** into a transition-state analogue of cytidine deamination.[24] Low micromolar inhibition constants were observed for several A3 variants.[21] However, because similar intrinsic preferences for deaminating cytosines preceded by thymine were observed for all A3 enzymes apart from A3G (Fig. 1C), there is uncertainty as to whether, or not, **dZ**-containing ssDNAs can selectively inhibit A3B in the context that no selective A3B inhibitors of any kind have been reported. Here we show that neighbouring nucleotides in ssDNA containing the inhibitor **dZ** strongly influence selectivity, allowing, in particular, selective targeting of A3B. This provides a platform for further development of oligonucleotide-inhibitors of A3 inhibitors as valuable probes for mechanistic and cellular studies, and, potentially, as adjuvants that suppress A3 mutagenesis in anticancer and anti-viral therapies.

Results and discussion

Hypothesis and methodology of this investigation

Although A3A and A3B favour deamination of the T**C** motif (underlined, bold C is deaminated) where the target dC is preceded by a thymidine, these enzymes also process cytidine in ssDNA with other adjacent nucleobases, but with lower efficiency (Fig. 1C).[25,26] For example, A3A and A3B are also capable of deaminating dC in the CCC sequence motif,[27] which is the most favoured motif for A3G. A3G and A3A preferentially deaminate dC at the 3′-end, denoted CC**C**,[25,28–31] with, respectively, at least 100 times and 5 times faster initial rate of deamination relative to other cytosines in the CCC-motif.[27] This is reflected in K_m values for catalytically active C-terminal domain of A3G ($A3G_{CTD}$, see explanation below): K_m (5′-ATT CC**C** AATT) ≈ 570 μM compared to K_m (5′-ATT C**C**dU AATT) ≈ 3.6 mM, where dU is 2′-deoxyuridine.[32] In contrast, A3B prefers dC at the 5′-end of this motif, denoted **C**CC,[26,27] with at least six-fold faster initial rate of deamination for this dC in comparison to the other cytosines.[27] Therefore, we hypothesized that replacing dC by **dZ** at the 5′ end of the **C**CC motif (**dZ**CC-Oligo, Table 1) would lead to a selective inhibitor of A3B, and conversely CC**dZ**-Oligo would inhibit A3A and A3G but not A3B.

To test our hypothesis we initially characterized kinetics of cytosine deamination by several A3 variants for a suboptimal substrate having the CCC-motif (CCC-oligo, Table 1). Here, we demonstrate that our A3 variants, A3A-mimic, $A3B_{CTD}$-DM and $A3G_{CTD}$, have the same deamination pattern on the CCC-motif reported previously for the wild-type enzymes (see Chart S2 in the ESI† for enzyme sequences). To evaluate the inhibitory potential of **dZ**-containing oligos we monitored the deamination of 5′-ATTT**C**ATTT by these A3 enzymes in the presence of potentially inhibitory oligos using the direct NMR-based assay.[21,32,33]

Evaluation of deamination of CCC-motif by various A3 constructs

GST-$A3G_{CTD}$ has a wild-type sequence of the catalytically active C-terminal domain of A3G. $A3B_{CTD}$-DM is a double mutant of the catalytically active C-terminal domain of A3B where two hydrophobic residues on the protein surface are replaced by

Table 1 Michaelis–Menten constants for A3 variants deaminating different DNA substrates measured by the ^{1}H-NMR assay (deaminated dC is in bold and underlined)[a]

		Enzymes		
Abbreviation	DNA sequence	A3A-mimic K_m, μM (k_{cat}, s^{-1})	$A3B_{CTD}$-DM K_m, μM (k_{cat}, s^{-1})	$A3G_{CTD}$ K_m, μM (k_{cat}, s^{-1})
TCA-oligo	5′-ATTT**C**ATTT	200 ± 30 (0.28 ± 0.04)	320 ± 60 (0.0080 ± 0.0014)	Not a substrate[b]
CCC-oligo	5′-ATT**C**C**C**AATT	440 ± 80 (0.38 ± 0.06)	Not a preferred substrate[c]	570 ± 90 (0.10 ± 0.04) (ref. 32)
	5′-ATT**C**CCAATT	Not a preferred substrate	590 ± 90 (0.009 ± 0.001)	Not a preferred substrate
dZCC-oligo	5′-ATT**dZ**C**C**AATT	520 ± 120 (0.44 ± 0.10)	Not a substrate	≈1 mM (≈0.1)
CC**dZ**-oligo	5′-ATT**C**C**dZ**AATT	Not a substrate	1370 ± 270 (0.0099 ± 0.0019)	Not a substrate

[a] A3A-mimic ($A3B_{CTD}$-QM-ΔL3-AL1swap, 50 nM) in pH 5.5 buffer and $A3B_{CTD}$-DM (2 μM) in pH 7.5 buffer consisting of 50 mM citrate-phosphate buffer, 200 mM NaCl and 2 mM β-mercaptoethanol. $A3G_{CTD}$ (850 nM) in pH 6.0 buffer consisting of 50 mM sodium phosphate, 1 mM citrate, 100 mM NaCl, 2 mM β-mercaptoethanol, 50 μM 4,4-dimethyl-4-silapentane-1-sulfonic acid (DSS). In all NMR assays, buffers contained 10% D_2O. K_m value for $A3G_{CTD}$ for CCC-oligo is stated for comparison with other enzymes and substrates. Uncertainties were calculated using standard error-propagation method. The cytidines that are not in bold and underlined were not deaminated in **dZ**-containing oligos over the time of the experiment. [b] "Not a substrate" means that none of dCs is deaminated under the experimental conditions reported. [c] "Not a preferred substrate" means that other dCs are also deaminated but at later time points when the concentration of the substrate with the preferred dC in the sequence decreased significantly due to deamination.

lysines (L230K and F308K) to enhance solubility (see Chart S3, ESI†).[21,34] Because these two mutations are located on the opposite side of the protein relative to the active site and do not belong to loop 1 and loop 7 responsible for substrate specificity,[27,29,34,35] they are unlikely to affect specificity, but some conflicting examples for other enzymes are known.[36–40] $A3B_{CTD}$-QM-ΔL3-AL1swap contains four mutations with loop 3 truncated and loop 1 of $A3B_{CTD}$ swapped with loop 1 of A3A, which constitute the main differences between amino acid sequences of A3A and $A3B_{CTD}$ (see Chart S2, ESI†).[21,34] This construct has the substrate specificity of A3A and provides a good contrast to $A3B_{CTD}$ in the context of the CCC motif.[27] That is why we refer to this enzyme as A3A-mimic.

Initially, we evaluated activity of our A3A-mimic and $A3B_{CTD}$-DM variants at different pH as very different optimum pH was reported for A3A and A3B.[27,41] In our hands, the optimum pH for A3A-mimic was 5.5 consistent with Ito *et al.*[41] However, $A3B_{CTD}$-DM is barely active at pH 5.5 but its activity increases with pH and reaches reasonable activity at pH 7.5 (see Chart S4 in ESI†). The optimum pH for $A3G_{CTD}$ used in our work was 6.0, which is consistent with previous reports.[27,32,41] Because even the remote mutations can sometimes affect the substrate specificity,[36–40] we then monitored the deamination of 5′-ATTCCCAATT (CCC-oligo, Fig. 2 and Table 1) by our A3 variants at the pH defined above. In line with previous observations,[27] A3A-mimic favoured the deamination of the third cytosine in the CC**C** motif (dC labelled 3, Fig. 2A). Product formation as a result of deamination of individual cytosines is easily detectable using ^{1}H NMR[21,32,33] because there is a good dispersion of H5 doublets (J = 8.5 Hz) of product uracils in corresponding sequences (see Chart S5 in the ESI†). This deamination pattern is similar to that reported previously for CC-preferring $A3G_{CTD}$, but with the qualifications that $A3G_{CTD}$ does not deaminate dC at the 5′ position (dC labelled 1, Fig. 2A) of the CCC-motif and has little enthusiasm for the middle C of the CCC motif: K_m (5′-ATT CC**C** AATT) ≈ 570 μM compared to K_m (5′-ATT C**C**dU AATT) ≈ 3.6 mM.[32] Deamination of only one dC at the beginning of the reaction is observed, indicating that dissociation of the enzyme from the oligo occurs between deamination events, since the concentration of substrate greatly exceeds concentration of enzyme.

In contrast to A3A-mimic, another enzyme variant, $A3B_{CTD}$-DM deaminated the first dC at the 5′ position of the **C**CC motif (Fig. 2B). The deamination products of other dCs were observed at later time-points and were always less intense in comparison with the signal of dU in position 1 indicating that deamination of non-preferred cytosines was incomplete during the experiment (2 h). The similar behaviour was observed previously for the wild type $A3B_{CTD}$.[27]

To exclude the possibility that substrate structure rather than sequence determines deamination patterns by A3[42,43] we evaluated our CCC-oligo using m-Fold[44] for possible formation of stem-loop structures. Two possible structures were proposed by m-Fold, both with positive unfavourable Gibbs free energy of formation (Chart S6, ESI†). Moreover, circular dichroism (CD) spectra recorded at pH 5.0, 6.0 and 7.2 showed no features indicating DNA secondary structure (Chart S7, ESI†). This establishes that the deamination patterns observed for the CCC-oligo with the different A3 enzymes are determined by the DNA sequence and not by the structure.

The Michaelis–Menten constants for the enzymes and ssDNA substrates used in this study are summarized in Table 1. Notably, the apparent binding affinity of $A3B_{CTD}$-DM and A3A-mimic for their preferred cytosines in the CCC motif (respectively, K_m ≈ 600 μM on **C**CC and K_m ≈ 400 μM on CC**C**) are weaker by a factor of 2 in comparison to the preferred T**C**A motif as previously reported ($A3B_{CTD}$-DM K_m ≈ 300 μM, A3A-mimic K_m ≈ 200 μM, Table 1).[21]

With respect to the substrate 5′-ATT CCC AATT, we can conclude that our A3 variants mimic the deamination pattern of

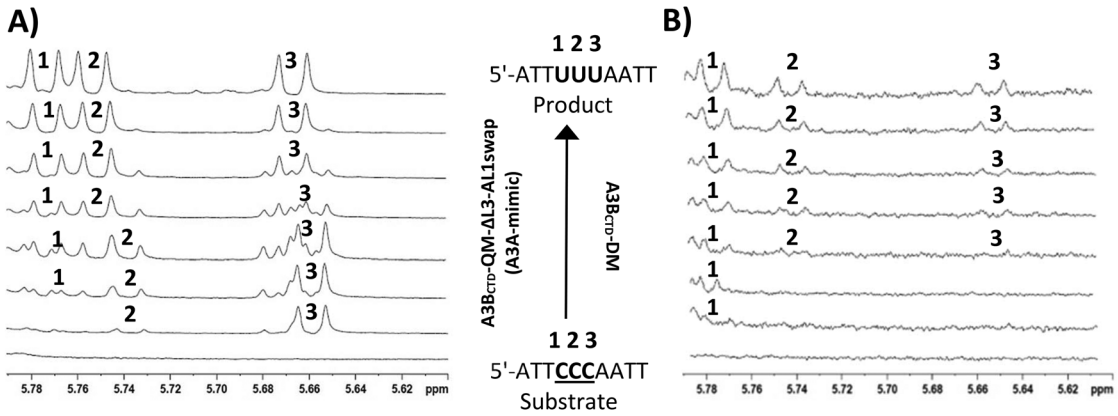

Fig. 2 ^{1}H-NMR spectra of preferential deamination of the CCC-oligo (800 μM) by A3A and A3B variants. Note that there is no signal in the uracil region of the ^{1}H-NMR spectra at the beginning of the reaction for the substrate. Spectra shown are recorded every 15 min. (A) $A3B_{CTD}$-QM-ΔL3-AL1swap (A3A-mimic, 2 μM) first deaminates dC at the 3′ position of the CC**C** in pH 5.5 buffer. Deamination of the resultant CCU species is nearly random, leading to multiple peaks at intermediate deamination for CUU, UCU and UUU species. (B) $A3B_{CTD}$-DM (2 μM) first deaminates dC at the 5′ position of the **C**CC motif in pH 7.5 buffer. dC at position 2 is next to be deaminated, followed by dC at position 3. Buffer is 50 mM citrate-phosphate, 200 mM NaCl, 2 mM β-mercaptoethanol, 200 μM DSS, 10% deuterium oxide.

wild-type A3A and $A3B_{CTD}$ in DNA substrates containing several cytosines. $A3B_{CTD}$ prefers a thymine in the 5′-position next to the target dC, whereas A3A preferentially accepts dC that is directly followed by purine (dA or dG) at the 3′-end. Nucleotides around the target dC are known to substantially influence substrate recognition by A3 enzymes.[18,27,45] Thus, we have a panel of A3 variants to test our hypothesis that we can selectively inhibit the catalytic activity of A3 enzymes by introducing **dZ** into different positions in the CCC sequence (**dZ**CC and CC**dZ**-oligos, Tables 1 and 2).

Evaluation of inhibitors

Next, we turned our attention to inhibitors based on the CCC-motif. Very recently, we had developed a micromolar inhibitor of A3 enzymes by incorporating **dZ** into their preferred deamination motif.[21] The T**dZ**A-oligo[21] (Table 2) did not significantly inhibit $A3G_{CTD}$. However, it targeted both A3A-mimic and $A3B_{CTD}$-DM with similar inhibition constants. To determine if we can selectively inhibit A3A-mimic, $A3B_{CTD}$-DM and $A3G_{CTD}$ enzymes, we synthesized CC**dZ** and **dZ**CC oligos using our previously established protocol[21] (see ESI† for experimental details). We used the TCA-oligo as a substrate to monitor the residual enzyme activity by NMR-based assay[21,32,33] in the presence of **dZ**-containing oligos because of its faster deamination than that of the CCC-oligo (Table 1). The NMR-based assay allows to obtain the initial velocity of deamination of the DNA substrates by A3 and consequently use the Michaelis–Menten kinetic model to characterize substrates and inhibitors of A3. To the best of our knowledge, all other *in vitro* A3 assays are indirect and rely on other enzymes with which DNA-based inhibitors may interact and provide false-positive or false-negative results. Moreover, **dZ** degrades in strong alkaline conditions,[46] which precludes evaluation of **dZ**-containing oligos as substrates of A3 in some indirect assays that use strong heat and base addition after the second enzymatic reaction using uracil-DNA glucosylase (UDG). Therefore, currently, the NMR-based direct assay is best suited to study DNA-based inhibitors of A3.

For an initial check, we analyzed deamination velocity by A3A-mimic and $A3B_{CTD}$-DM at specific concentration of inhibitors, which provides qualitative information about A3-selectivity of our inhibitors. Consistent with our hypothesis, CC**dZ**-oligo significantly inhibits deamination of substrate 5′-ATTTCATTT by A3A-mimic (Fig. 3A), as well as by $A3G_{CTD}$ (as previously reported in ref. 21), but not $A3B_{CTD}$-DM (Fig. 3A and Table 2). In contrast, **dZ**CC-oligo inhibits substrate deamination by $A3B_{CTD}$-DM variant (Fig. 3B) but has no measureable effect on the initial velocity of A3A-mimic (Fig. 3A, **dZ**CC) or $A3G_{CTD}$. To ensure that the inhibitor is not processed by the inhibited enzyme we checked NMR spectrum of CC**dZ**-oligo in the presence of A3A-mimic, which is the most active deaminase in our set of A3. No changes in NMR spectrum were observed over 3.7 hours and, most importantly, no signals from uridine appeared in the range of 5.5–6.0 ppm (see Chart S18, ESI†). This confirms that A3A specifically recognizes **dZ** in CC**dZ**-oligo and does not deaminate other dCs in this motif in excess of oligo relative to the enzyme.

To quantitatively characterize the extent of inhibition we analyzed the linear dependence of inverse deamination speed on inhibitor concentration and obtained inhibition constants (K_i, Fig. 3C, D and Table 2) based on a competitive mode of inhibition.[21] K_i values of the selective **dZ**-oligos on A3A-mimic and $A3B_{CTD}$-DM variants (Fig. 3C, D and Table 2) indicate approximately two-fold weaker inhibition than the K_i of our previously reported essentially non-selective T**dZ**A inhibitor.[21] This is consistent with the two-fold weaker K_m of the CCC oligo to these enzymes in comparison with K_m's for the preferred TCA-oligo (Table 1). Nevertheless, we see a thirty-fold increase in apparent affinity (K_m/K_i) because **dZ** is placed in the ssDNA CCC sequence instead of the preferred dC.

To evaluate the scenario where **dZ**CC/CC**dZ**-inhibitors are deaminated by other A3 enzymes, we used **dZ**CC- and CC**dZ**-oligos as substrates and determined K_m values for non-preferred enzymes A3A-mimic/$A3G_{CTD}$ and $A3B_{CTD}$-DM, respectively. The **dZ**CC-oligo, which is an inhibitor of $A3B_{CTD}$-DM but not of A3A-mimic and $A3G_{CTD}$, is a worse substrate for these latter two enzymes than TCA-oligo (Table 1, K_m = 520 ± 90 μM for A3A-mimic and $K_m \approx 1$ mM for $A3G_{CTD}$). More markedly, CC**dZ**-oligo, which inhibits A3A-mimic and $A3G_{CTD}$, is a very poor substrate for $A3B_{CTD}$-DM with $K_m \approx$ 1370 ± 270 μM (Table 1). By comparing the K_m value for **dZ**CC-oligo deaminated by A3A-mimic (K_m = 520 μM, which is the lowest K_m value for **dZ**-oligos as substrates to A3A-mimic reported here) with the K_i value for $A3B_{CTD}$-DM (K_i = 18.5 μM) by the same oligo (K_m/K_i = 30), we can conclude that inhibition of $A3B_{CTD}$-DM will prevail over deamination by A3A-mimic.

Table 2 Inhibition constants (K_i, μM) for A3 variants measured by the NMR-based assay[a]

		Enzymes		
Abbreviation	DNA sequence	A3A (mimic)	$A3B_{CTD}$-DM	$A3G_{CTD}$
T**dZ**A-Oligo	5′-ATTT**dZ**ATTT	7.5 ± 1.7[b]	11.4 ± 2.6[b]	Not an inhibitor[b]
CC**dZ**-Oligo	5′-ATTCC**dZ**AATT	12.3 ± 1.8	Not an inhibitor	53 ± 10[b]
dZCC-Oligo	5′-ATT**dZ**CCAATT	Not an inhibitor	18.5 ± 5.5	Not an inhibitor

[a] See conditions reported in Table 1. [b] See ref. 21, K_i values are provided for comparison; all experiments were repeated multiple times in the same laboratory and the same time interval.

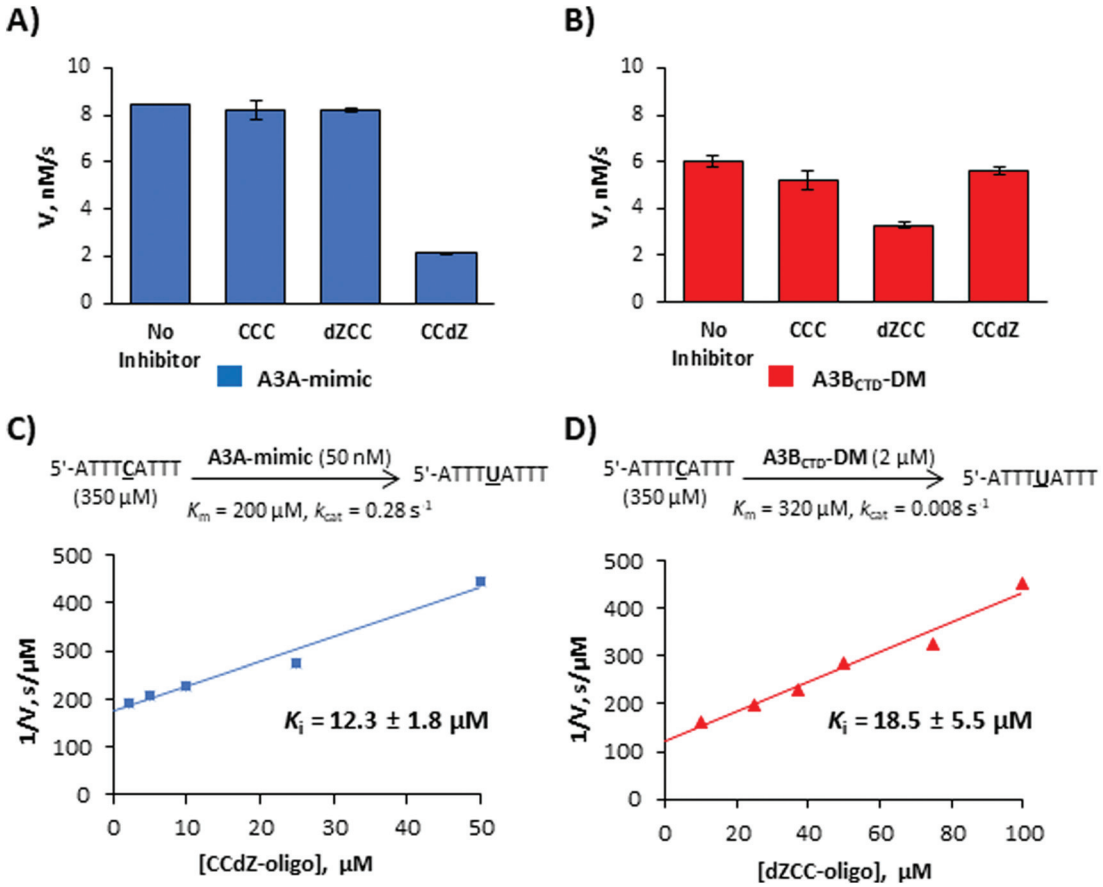

Fig. 3 Selective inhibition of A3 enzymes by **dZ**-containing ssDNAs. (A) and (B) Deamination of 5′-ATTTCATTT (TCA-oligo, 350 μM) in the absence and presence of potential inhibitors (50 μM ssDNA CCC-oligo, **dZ**CC-oligo and CC**dZ**-oligo). (A) A3A-mimic (A3B$_{CTD}$-QM-ΔL3-AL1swap, 50 nM). (B) A3B$_{CTD}$-DM (2 μM). (C) Inhibition of deamination of the TCA substrate by A3A-mimic in the presence of various concentrations of CC**dZ**-oligo. (D) Inhibition of deamination of the TCA substrate by A3B$_{CTD}$-DM in the presence of various concentrations of **dZ**CC-oligo.

Conclusions

Taking advantage of the discrimination pattern for deamination of the CCC motif by A3A/A3G compared to A3B,[27] we incorporated our previously reported inhibitor of cytidine deamination, 2′-deoxyzebularine (**dZ**), in different positions in the CCC-motif. Incorporation of **dZ** in place of preferentially deaminated dC led to the first inhibitors capable of selectively targeting the catalytic activity of individual members of the A3 family, especially cancer-associated A3B variant. Comparison of the A3B$_{CTD}$-DM inhibition constant (K_i) for **dZ**CC (Table 2) to K_m values for **dZ**CC deamination of the target dC by A3A-mimic and A3G$_{CTD}$ (Table 1) indicates at least 30-fold higher apparent binding to A3B$_{CTD}$-DM than to other enzymes. This means that **dZ**CC-oligo is an inhibitor of A3B$_{CTD}$-DM rather than a substrate of A3A-mimic and A3G$_{CTD}$. **dZ**CC-oligo should not be deaminated by A3B$_{CTD}$-DM, which it inhibits, because $K_i \ll K_m$ for the remaining cytidines. Our data illustrate this argument because CC**dZ**-oligo is an inhibitor of A3A-mimic and it is not deaminated by the same enzyme, which indicates that A3A-mimic strongly prefers to bind to **dZ** rather than to either dC in the oligo. To our knowledge, **dZ**CC-oligo is the first reported selective inhibitor of A3B$_{CTD}$, although the selective small-molecule A3G inhibitors have been reported.[47,48] Inhibition of full-length two-domain A3B and A3G enzymes and the cellular effect of our inhibitors still need to be determined, but we expect longer oligonucleotides to maintain similar inhibition patterns since binding to the catalytically inactive N-terminal domains has been established as non-specific.[49–51] The use of more powerful inhibitors of cytidine deamination than **dZ** is expected to increase inhibition to the level required for the cellular studies. For CC**dZ**-oligo, different inhibition constants against A3A-mimic and A3G$_{CTD}$ indicate potential for further discrimination between these enzymes. Other DNA sequences that have been shown to be deaminated differently by A3A and A3B[18,35,43,52] can also be evaluated as alternative starting points for the design of A3-selective inhibitors in future. Our **dZ**-oligos do not inhibit CDA as CDA accepts only individual nucleosides not oligonucleotides.[53] Similarly, we do not expect our inhibitors to inhibit DNA methyltransferases[54] because these enzymes recognise flipped out cytosines in double-stranded DNA not in single-stranded DNA.[55] Nevertheless, we plan to test our inhibitors in normal cells as control for unanticipated cytotoxicity at later stage.

Overall, our work provides a platform for development of more potent and selective A3-inhibitors with the ultimate goal to be used for cellular studies and as possible adjuvants in anti-viral and anti-cancer treatments.

Material and methods

Detailed methods are provided in the ESI.†

Synthesis of oligonucleotides containing 2′-deoxyzebularine (dZ)

2′-Deoxyzebularine phosphoramidite was prepared as described previously.[21] Synthetic procedures are provided in ESI.†

Protein expression and purification

Expression and purification procedures are provided in ESI.† A3B C-terminal domain (residues 187 to 378) protein variants $A3B_{CTD}$-QM-ΔL3-AL1swap (termed A3A-mimic) and $A3B_{CTD}$-DM, and GST-fused A3G C-terminal domain (residues 191 to 384) protein variant $A3G_{CTD}$ were prepared as described previously.[32,34]

Kinetic characterization of deamination activity using NMR-based assay

Kinetic characterization of A3 protein variants ($A3B_{CTD}$-QM-ΔL3-AL1swap, $A3B_{CTD}$-DM, and $A3G_{CTD}$) on preferred cytidine in 5′-ATTCCCAATT, 5′-ATT**dZ**CCAATT, and 5′-ATTCC**dZ**AATT substrates were evaluated using an established NMR-based assay[21,32,33] as described in ESI.†

Evaluation of inhibitors in NMR-based assay

The NMR-based inhibition assay as described previously[21,32] was conducted on 350 μM 5′-ATTTCATTT substrate with A3 variants in the presence of **dZ**-containing oligodeoxynucleotides. Procedures and inhibition constants calculation are provided in ESI.†

Conflicts of interest

There are no conflicts to declare.

Funding

We are grateful for the financial support provided by the Worldwide Cancer Research (grant 16-1197), Massey University Research Fund (MURF 2015, 7003) and School of Fundamental Sciences, Massey University. Funding for open access charge: Worldwide Cancer Research (grant APC-19-0007).

Acknowledgements

NMR and mass-spectrometry facilities at Massey University and the assistance of Dr P. J. B. Edwards and D. Lun are gratefully acknowledged. We thank Prof. Reuben S. Harris (University of Minnesota, USA) and members of his cancer research program for helpful discussions.

References

1 R. S. Harris and J. P. Dudley, *Virology*, 2015, **479–480**, 131–145.
2 S. G. Conticello, C. J. F. Thomas, S. K. Petersen-Mahrt and M. S. Neuberger, *Mol. Biol. Evol.*, 2005, **22**, 367–377.
3 R. S. Harris and M. T. Liddament, *Nat. Rev. Immunol.*, 2004, **4**, 868–877.
4 R. S. LaRue, V. Andrésdóttir, Y. Blanchard, S. G. Conticello, D. Derse, M. Emerman, W. C. Greene, S. R. Jónsson, N. R. Landau, M. Löchelt, H. S. Malik, M. H. Malim, C. Münk, S. J. O'Brien, V. K. Pathak, K. Strebel, S. Wain-Hobson, X.-F. Yu, N. Yuhki and R. S. Harris, *J. Virol.*, 2009, **83**, 494–497.
5 T. Izumi, K. Shirakawa and A. Takaori-Kondo, *Mini-Rev. Med. Chem.*, 2008, **8**, 231–238.
6 R. Suspene, M.-M. Aynaud, D. Guetard, M. Henry, G. Eckhoff, A. Marchio, P. Pineau, A. Dejean, J.-P. Vartanian and S. Wain-Hobson, *Proc. Natl. Acad. Sci. U. S. A.*, 2011, **108**, 4858–4863.
7 C. Swanton, N. McGranahan, G. J. Starrett and R. S. Harris, *Cancer Discovery*, 2015, **5**, 704–712.
8 E.-Y. Kim, R. Lorenzo-Redondo, S. J. Little, Y.-S. Chung, P. K. Phalora, I. Maljkovic Berry, J. Archer, S. Penugonda, W. Fischer, D. D. Richman, T. Bhattacharya, M. H. Malim and S. M. Wolinsky, *PLoS Pathog.*, 2014, **10**, e1004281.
9 S. Venkatesan, R. Rosenthal, N. Kanu, N. McGranahan, J. Bartek, S. A. Quezada, J. Hare, R. S. Harris and C. Swanton, *Ann. Oncol.*, 2018, **29**, 563–572.
10 E. K. Law, A. M. Sieuwerts, K. LaPara, B. Leonard, G. J. Starrett, A. M. Molan, N. A. Temiz, R. I. Vogel, M. E. Meijer-van Gelder, F. C. G. J. Sweep, P. N. Span, J. A. Foekens, J. W. M. Martens, D. Yee and R. S. Harris, *Sci. Adv.*, 2016, **2**, e1601737.
11 J. Zou, C. Wang, X. Ma, E. Wang and G. Peng, *Cell Biosci.*, 2017, **7**, 29.
12 A. M. Sieuwerts, S. Willis, M. B. Burns, M. P. Look, M. E. Meijer-Van Gelder, A. Schlicker, M. R. Heideman, H. Jacobs, L. Wessels, B. Leyland-Jones, K. P. Gray, J. A. Foekens, R. S. Harris and J. W. M. Martens, *Horm. Cancer*, 2014, **5**, 405–413.
13 P. J. Vlachostergios and B. M. Faltas, *Nat. Rev. Clin. Oncol.*, 2018, **15**, 495–509.
14 L. Galluzzi and I. Vitale, *Trends Genet.*, 2017, **33**, 491–492.
15 M. B. Burns, N. A. Temiz and R. S. Harris, *Nat. Genet.*, 2013, **45**, 977–983.
16 J. M. Kidd, T. L. Newman, E. Tuzun, R. Kaul and E. E. Eichler, *PLoS Genet.*, 2007, **3**, 584–592.
17 M. E. Olson, R. S. Harris and D. A. Harki, *Cell Chem. Biol.*, 2018, **25**, 36–49.
18 K. Chan, S. A. Roberts, L. J. Klimczak, J. F. Sterling, N. Saini, E. P. Malc, J. Kim, D. J. Kwiatkowski, D. C. Fargo, P. A. Mieczkowski, G. Getz and D. A. Gordenin, *Nat. Genet.*, 2015, **47**, 1067–1072.
19 M. B. Burns, L. Lackey, M. A. Carpenter, A. Rathore, A. M. Land, B. Leonard, E. W. Refsland, D. Kotandeniya,

N. Tretyakova, J. B. Nikas, D. Yee, N. A. Temiz, D. E. Donohue, R. M. McDougle, W. L. Brown, E. K. Law and R. S. Harris, *Nature (London, U. K.)*, 2013, **494**, 366–370.

20 B. Leonard, J. L. McCann, G. J. Starrett, L. Kosyakovsky, E. M. Luengas, A. M. Molan, M. B. Burns, R. M. McDougle, P. J. Parker, W. L. Brown and R. S. Harris, *Cancer Res.*, 2015, **75**, 4538–4547.

21 M. V. Kvach, F. M. Barzak, S. Harjes, H. A. M. Schares, G. B. Jameson, A. M. Ayoub, R. Moorthy, H. Aihara, R. S. Harris, V. V. Filichev, D. A. Harki and E. Harjes, *Biochemistry*, 2019, **58**, 391–400.

22 S. Xiang, S. A. Short, R. Wolfenden and C. W. Carter, *Biochemistry*, 1995, **34**, 4516–4523.

23 J. J. Barchi, A. Haces, V. E. Marquez and J. J. McCormack, *Nucleosides Nucleotides*, 1992, **11**, 1781–1793.

24 C. H. Borchers, V. E. Marquez, G. K. Schroeder, S. A. Short, M. J. Snider, J. P. Speir and R. Wolfenden, *Proc. Natl. Acad. Sci. U. S. A.*, 2004, **101**, 15341–15345.

25 M. D. Stenglein, M. B. Burns, M. Li, J. Lengyel and R. S. Harris, *Nat. Struct. Mol. Biol.*, 2010, **17**, 222–229.

26 I.-J. L. Byeon, J. Ahn, M. Mitra, C.-H. Byeon, K. Hercik, J. Hritz, L. M. Charlton, J. G. Levin and A. M. Gronenborn, *Nat. Commun.*, 2013, **4**, ncomms2883.

27 I.-J. L. Byeon, C.-H. Byeon, T. Wu, M. Mitra, D. Singer, J. G. Levin and A. M. Gronenborn, *Biochemistry*, 2016, **55**, 2944–2959.

28 M. A. Carpenter, E. Rajagurubandara, P. Wijesinghe and A. S. Bhagwat, *DNA Repair*, 2010, **9**, 579–587.

29 A. Rathore, M. A. Carpenter, O. Demir, T. Ikeda, M. Li, N. M. Shaban, E. K. Law, D. Anokhin, W. L. Brown, R. E. Amaro and R. S. Harris, *J. Mol. Biol.*, 2013, **425**, 4442–4454.

30 R. M. Kohli, S. R. Abrams, K. S. Gajula, R. W. Maul, P. J. Gearhart and J. T. Stivers, *J. Biol. Chem.*, 2009, **284**, 22898–22904.

31 R. M. Kohli, R. W. Maul, A. F. Guminski, R. L. McClure, K. S. Gajula, H. Saribasak, M. A. McMahon, R. F. Siliciano, P. J. Gearhart and J. T. Stivers, *J. Biol. Chem.*, 2010, **285**, 40956–40964.

32 S. Harjes, W. C. Solomon, M. Li, K.-M. Chen, E. Harjes, R. S. Harris and H. Matsuo, *J. Virol.*, 2013, **87**, 7008–7014.

33 A. Furukawa, T. Nagata, A. Matsugami, Y. Habu, R. Sugiyama, F. Hayashi, N. Kobayashi, S. Yokoyama, H. Takaku and M. Katahira, *EMBO J.*, 2009, **28**, 440–451.

34 K. Shi, M. A. Carpenter, K. Kurahashi, R. S. Harris and H. Aihara, *J. Biol. Chem.*, 2015, **290**, 28120–28130.

35 K. Shi, M. A. Carpenter, S. Banerjee, N. M. Shaban, K. Kurahashi, D. J. Salamango, J. L. McCann, G. J. Starrett, J. V. Duffy, O. Demir, R. E. Amaro, D. A. Harki, R. S. Harris and H. Aihara, *Nat. Struct. Mol. Biol.*, 2017, **24**, 131–139.

36 V. Weinreb, L. Li, S. N. Chandrasekaran, P. Koehl, M. Delarue and C. W. Carter Jr., *J. Biol. Chem.*, 2014, **289**, 4367–4376.

37 G. Yang, N. Hong, F. Baier, C. J. Jackson and N. Tokuriki, *Biochemistry*, 2016, **55**, 4583–4593.

38 B. Song, Y. Yue, T. Xie, S. Qian and Y. Chao, *Mol. Biotechnol.*, 2014, **56**, 232–239.

39 M. Schmidt, D. Hasenpusch, M. Kähler, U. Kirchner, K. Wiggenhorn, W. Langel and U. T. Bornscheuer, *ChemBioChem*, 2006, **7**, 805–809.

40 P. Oelschlaeger, S. L. Mayo and J. Pleiss, *Protein Sci.*, 2005, **14**, 765–774.

41 F. Ito, Y. Fu, S. A. Kao, H. Yang and X. S. Chen, *J. Mol. Biol.*, 2017, **429**, 1787–1799.

42 C. M. Holtz, H. A. Sadler and L. M. Mansky, *Nucleic Acids Res.*, 2013, **41**, 6139–6148.

43 T. V. Silvas, S. Hou, W. Myint, E. Nalivaika, M. Somasundaran, B. A. Kelch, H. Matsuo, N. Kurt Yilmaz and C. A. Schiffer, *Sci. Rep.*, 2018, **8**, 7511.

44 M. Zuker, *Nucleic Acids Res.*, 2003, **31**, 3406–3415.

45 J. W. Rausch, L. Chelico, M. F. Goodman and S. F. J. Le Grice, *J. Biol. Chem.*, 2009, **284**, 7047–7058.

46 M. Vives, R. Eritja, R. Tauler, V. E. Marquez and R. Gargallo, *Biopolymers*, 2004, **73**, 27–43.

47 M. Li, S. M. D. Shandilya, M. A. Carpenter, A. Rathore, W. L. Brown, A. L. Perkins, D. A. Harki, J. Solberg, D. J. Hook, K. K. Pandey, M. A. Parniak, J. R. Johnson, N. J. Krogan, M. Somasundaran, A. Ali, C. A. Schiffer and R. S. Harris, *ACS Chem. Biol.*, 2012, **7**, 506–517.

48 M. E. Olson, M. Li, R. S. Harris and D. A. Harki, *ChemMedChem*, 2013, **8**, 112–117.

49 Y. Iwatani, H. Takeuchi, K. Strebel and J. G. Levin, *J. Virol.*, 2006, **80**, 5992–6002.

50 F. Navarro, B. Bollman, H. Chen, R. Konig, Q. Yu, K. Chiles and N. R. Landau, *Virology*, 2005, **333**, 374–386.

51 J. D. Salter and H. C. Smith, *Trends Biochem. Sci.*, 2018, **43**, 606–622.

52 M. Liu, A. Mallinger, M. Tortorici, Y. Newbatt, M. Richards, A. Mirza, R. L. M. van Montfort, R. Burke, J. Blagg and T. Kaserer, *ACS Chem. Biol.*, 2018, **13**, 2427–2432.

53 C. B. Yoo, S. Jeong, G. Egger, G. Liang, P. Phiasivongsa, C. Tang, S. Redkar and P. A. Jones, *Cancer Res.*, 2007, **67**, 6400–6408.

54 V. E. Marquez, J. A. Kelley, R. Agbaria, T. Ben-Kasus, J. C. Cheng, C. B. Yoo and P. A. Jones, *Ann. N. Y. Acad. Sci.*, 2005, **1058**, 246–254.

55 S. S. Smith, B. E. Kaplan, L. C. Sowers and E. M. Newman, *Proc. Natl. Acad. Sci. U. S. A.*, 1992, **89**, 4744–4748.